

Novel Application of Neutrinos to Evaluate U.S. Nuclear Weapons Performance

J.R. Distel, E.C. Dunton, J.M. Durham, A.C. Hayes, W.C. Louis, J.D. Martin, G.W. Misch, M.R. Mumpower, Z. Tang, R.T. Thornton, B.T. Turner, R.G. Van De Water, and W.S. Wilburn
Los Alamos National Laboratory, Los Alamos, New Mexico, 87545, USA

There is a growing realization that neutrinos can be used as a diagnostic tool to better understand the inner workings of a nuclear weapon. Robust estimates demonstrate that an Inverse Beta Decay (IBD) neutrino scintillation detector built at the Nevada Test Site of 1000-ton active target mass at a standoff distance of 500 m would detect thousands of neutrino events per kTe of nuclear yield ^a. This would provide less than 4% statistical error on measured neutrino rate and 5% error on neutrino energy. Extrapolating this to an error on the test device explosive yield requires knowledge from evaluated nuclear databases, non-equilibrium fission rates, and assumptions on internal neutron fluxes. Initial calculations demonstrate that prompt neutrino rates from a short pulse of ²³⁹Pu fission is about a factor of two less than that from a steady state assumption. As well, there are significant energy spectral differences as a function of time after the pulse that needs to be considered. These and other model dependencies will be discussed further in the paper. In the absence of nuclear weapons testing, many of the technical and theoretical challenges of a full nuclear test could be mitigated with a low cost smaller scale 20 ton fiducial mass IBD demonstration detector placed near a pulsed reactor. Potential reactors include the Texas A&M University (TAMU) TRIGA 1GW-10 millisecond pulsed facility or the Sandia Annular Core Research Reactor. The short duty cycle and repeatability of pulses would provide critical real environment testing and measurements which would be valuable for planning a possible real test shot in the future. Furthermore, the neutrino rate as a function of time data would provide unique constraints on fission databases and equilibrium assumptions. Finally, there are impactful science drivers such as sensitive searches for ~ 1 eV² sterile neutrinos and \sim MeV scale axions.

I. INTRODUCTION

In this paper, we discuss the feasibility of diagnosing a potential U.S. nuclear weapons test using a neutrino detector. This idea was first proposed in 1953 by Reines and Cowan [1, 2] to observe the then hypothesized neutrino. Since then, the neutrino was discovered [3] and over the decades the field of neutrino research has matured and many properties of the neutrino have been measured such as interaction cross sections, masses, abundances, etc [4]. The neutrino has been observed from the sun, supernova, nuclear reactors, accelerators, and even the Earth's core. Interestingly, one of the most prolific sources of neutrinos, a man-made nuclear explosion, has yet to be detected.

Frederick Reines and Clyde Cowan, Jr. were the first physicists to understand the utility of a nuclear weapon test to produce a prolific source of neutrinos in a relatively short time window and reasonable stand off distance, as shown in Fig.1. Such a concept was proposed at LANL in the 1950's [2, 5] but was finally rejected for a more controlled experiment at a nuclear reactor [1, 3] – this latter method went on to win the 1995 Nobel prize in physics for the detection of the neutrino. What they maybe did not realize at the time is that continual improvements in neutrino detector technology over the decades could one day have many applications to LANL's main mission more than 70 years later.

The application that we will be exploring in this paper is the use of a \sim 1000-ton scale Inverse Beta Decay (IBD) neutrino detector to measure the nuclear weapon performance at a safe stand off distance. Situating the detector at a central accessible point allows it to be re-used for multiple shots. A 500 m standoff distance is sufficient to insulate the detector from shock waves but close enough to potentially detect thousands of neutrinos. The detector should be at least 10 m underground to shield from cosmic ray backgrounds. First, we perform robust rate calculations for neutrinos from a hypothetical yield to indicate if the concept is feasible. We have estimated the neutrino flux and neutrino event rates from a weapon test as a function of energy and time and have estimated fission fluxes by assuming a single prompt fission event which generates fragments with a known independent yield distribution. These products decay to a distribution of isotopes and the resulting neutrino spectrum is folded with known neutrino cross sections to produce rates for IBD. As well, a discussion of systematic errors associated with extrapolating the measured neutrino rates to nuclear detonation yield will be presented.

Second, the proven detection method for neutrinos from power reactors (U or Pu fission) is a large mass liquid scintillator detector (>100 -tons) that measures the IBD channel via $\bar{\nu}_e + p \rightarrow n + e^+$ [6]. The detection of the prompt positron followed by gamma rays from neutron capture provides a very powerful signal with excellent background

^a we use the convention kTe for kilo-tons of explosive yield, while for neutrino detector mass we use ton.

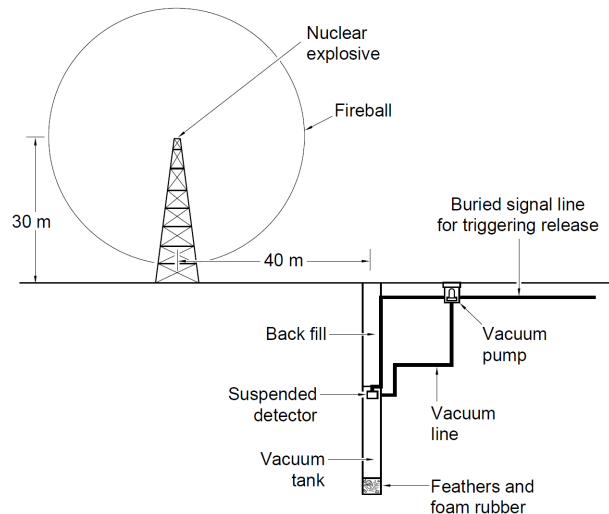


FIG. 1. Original proposed experiment by Reines and Cowan for the detection of the elusive neutrino. The proposed experiment is approximately 90 meters away from the nuclear explosion, necessitating a complex drop mechanism to prevent destruction of the detector before detection of the neutrinos can be achieved. The figure is reproduced from [2].

rejection. The reconstructed positron interaction preserves the original neutrino energy and the event time to the nano-second level. Thus, the neutrino flux rate, energy, and time distribution can be accurately reconstructed. Initial straight forward rate estimates demonstrates that a large 1000-ton-scale detector 500 m from the nuclear test device will have significant event rates. We expect that neutrino rates can be measured with an uncertainty of four percent or better and energy at the $\sim 5\%$ level. These robust detectors might be the key to detecting neutrinos with sufficient rate, energy, and time resolution to determine weapon yield and other parameters of interest to U.S. weapons design community.

Finally, we will discuss plans to test a small 25-ton IBD detector at a pulsed reactor facility. The aim is three fold; 1) test experimental issues operating a IBD detector at a pulsed fission source, 2) measure, for the first time, the neutrino time and energy distributions from a pulsed source, and 3) evaluate yield systematic errors from a pulsed non-equilibrium fission source using measured neutrino rates. This will be followed up by discussing possible fundamental and applied physics that can be accomplished by such a prototype detector at a pulsed reactor.

II. ESTIMATED DETECTED NEUTRINO EVENT RATES FROM A POTENTIAL NUCLEAR WEAPONS TEST

The fission processes produce neutrinos throughout the fission decay chain, which summed up total about ~ 2.5 antineutrinos per U or Pu fission decay assuming non-equilibrium conditions of a fast fission pulse as described in Section III. For a steady state nuclear reactor this number is about ~ 6 antineutrinos per fission [7]. This difference is significant and needs to be better understood and measured.

Detailed flux calculations are readily available and show antineutrino spectra up to about 10 MeV [8]. Once produced, the neutrinos are emitted isotropically and most will pass through the Earth. However, with a sizable scintillation detector filled with hydrogen (such as mineral oil - CH_2), some of the neutrinos can interact through the inverse beta decay mechanism, producing a time correlated positron and neutron in the final state that can be detected. Due to the threshold of 1.806 MeV for the reaction, the maximum energy the positron can deposit is ~ 8 MeV in the form of scintillation and Cherenkov light in the detector medium. If the detector is doped with Gd, then the final state neutron thermalizes quickly and captures on the Gd within 10's of micro-seconds producing up to ~ 8 MeV of gamma-rays [9]. This time coincidence of the positron and neutron capture signals are unique and provide powerful rejection of random backgrounds.

Decades of development of neutrino detectors to measure neutrino properties from nuclear reactors has produced a proven and robust design to detect neutrino IBD interactions [10, 11]. The basic detector design is a large volume (10 to 10,000 tons) of optically transparent scintillator material surrounded by large number of Photo-Multiplier Tubes (PMT's) that detect the scintillation light from particle interactions. Fast digitizer electronics are used to read out the PMT's which allows reconstruction of neutrino event rates, energy, position, and time of arrival. The next two

sub-sections present neutrino IBD rate calculations for a mineral oil based detector instrumented with hundreds of PMT's. We start with simple back of the envelope easy to understand calculations then move up to more complete calculations folding flux and cross sections with efficiency, ensuring consistency along the way.

1. Back of the Envelope

The IBD neutrino event rate is given by $N_\nu = \phi_\nu \sigma N_{freeH}$. The flux average IBD cross section σ is roughly 0.5×10^{-42} cm² for a typical U or Pu fission decay neutrino flux [12]. The neutrino flux ϕ_ν from a burst is estimated easily from energy considerations where 1 kTe of TNT = 4.2×10^{12} J = 2.6×10^{25} MeV of energy. With about 200 MeV/fission, this yields 1.3×10^{23} fissions. Including a factor of 2.5 for the average number of neutrinos per fission from a pulse of fast neutrons, as described in Section III [12], this gives about half a mole of neutrinos per 1 kTe. Assuming half a mole of neutrino fissions in one burst lasting 1000 seconds at a distance of 500 m, gives a neutrino flux average of $\phi_\nu = 0.95 \times 10^{13}$ ν cm⁻². A distance of 500 m was considered a reasonable standoff distance for insuring detector integrity, assuming both the blast and detector are buried underground. The number of free H in one metric ton of neutrino detector mineral oil is 8.6×10^{28} atoms. Putting these three numbers together gives an IBD neutrino rate of 0.41 events/kTe/ton at 500 m. This is assuming 100% efficiency. However, the reaction threshold for neutrino IBD reactions results in a 50% cross section efficiency above this energy. The detector reconstruction efficiency is estimated to be about 80% (see subsection IV 5), which results in a basic efficiency corrected neutrino rate of 0.16 events/kTe/ton at 500 m. This translates into thousands of detected neutrino events for a 1000-ton medium sized neutrino detector at a distance of 500 m from a plausible nuclear test. As well as rate, an IBD detector would be able to determine neutrino energy better than 5% resolution and event arrival time to nano-second level.

2. Spectrum Folding Calculations

A more detailed calculation of event rates is performed by folding the time dependent spectrum of neutrinos produced by fission products with the cross section for inverse β decay. As an example, we take the energy spectrum of $\bar{\nu}$ produced by fission products of ²³⁹Pu from Ref. [13] and Section III. We calculate the time dependent isotope yields after the prompt fission event, and show the time-integrated neutrino energy spectra in several windows of time after the fission pulse in the right panels of Fig. 2. The IBD energy threshold results in loss of sensitivity to the neutrino spectrum below the 1.8 MeV threshold, which is $\approx 50\%$ of all generated neutrinos (hence, $\approx 50\%$ cross section threshold efficiency). The total time-integrated neutrino spectrum, folded over the IBD cross section, is shown in the left panel of Fig. 2, while the right panel shows the spectrum for different time intervals. This shows that on average higher energy neutrinos come in the earliest time bins after the prompt fission pulse.

A detector with 1000-tons of active mass would have a radius of ~ 6 m. Such an instrument placed 500 m from a test device subtends a fraction of 3.6×10^{-5} of the solid angle of the neutrinos emitted by the device. A typical Gd-doped mineral oil produced by Eljen, EJ-335, [14], has a hydrogen density of 6×10^{22} H atoms per cubic centimeter. This gives an event rate of 0.16 events/kTe/ton, similar to the back-of-the-envelope calculation quoted above. Uncertainties associated with the IBD cross section can be evaluated in future work, but are expected to be less than $\sim 1\%$. Due to the threshold and rising neutrino cross section, the detectable neutrino energy spectrum shown in Figure 2 peaks around ~ 4 MeV, with an endpoint energy near 8 MeV. Figure 3 shows the neutrino production rate from a short fission burst, with approximately 30% of the total neutrinos arriving before 10 seconds, though there is a long tail up to 100's of seconds.

III. MEASUREMENTS, EXTRACTION OF NUCLEAR TEST YIELD, SYSTEMATIC ERRORS

1. Extracting fission yields from the emitted neutrinos

Reactor thermal fission neutrino spectra are known at the peak of the spectrum when folded with the IBD cross section to an accuracy of approximately 3%, however the uncertainties are energy dependent and at the largest energies (above approximately 8 MeV) the uncertainty is approximately 20% [15]. In a nuclear explosion, the neutron energies are considerably higher than in a reactor where the neutrons inducing fission in a nuclear explosion are fast neutrons (with energies of ~ 0.4 -2.0 MeV) and 14 MeV neutrons. Extrapolating from measured reactor thermal spectra to those expected for weapons-relevant neutron energies, with reasonable accuracy, is made possible by the very detailed systematic studies of the energy-dependence of both the independent and cumulative fission product yields

	0.0-0.1 s	0.1-1.0 s	1.0-10.0 s	10.0-100.0 s	100.0-1000.0 s	Total
$N_{\bar{\nu}}$ (Fast)	0.020	0.145	0.572	0.890	0.864	2.491
$N_{\bar{\nu}}$ (14 MeV)	0.018	0.129	0.479	0.697	0.707	2.03

TABLE I. Total number of antineutrinos over all energy per fission emitted in each window of time (columns) by ^{239}Pu fission induced by fast neutrons (top rows) and by 14 MeV neutrons (bottom rows). These quantities represent the total normalizations extracted from the curves presented in the right panel of Figure 2.

(FPYs) that have been carried out at Los Alamos and elsewhere, in a joint long-term experimental and theoretical program [16].

The spectra of neutrinos emitted by the decay of fission products generated by fast and 14 MeV neutrons are nearly equal in shape, but can be differentiated by their total magnitudes. To see this, we assume that the fission event occurs in an extremely short duration at early time and then track the subsequent beta decays of all isotopes produced by the immediate fission event and the subsequent decays. Using the time-dependent yields of the various unstable isotopes, we compute the evolution of the spectrum up to 10^3 seconds after the initial fission. The process by which this computation is performed is discussed further in the next subsection.

In the left panel of Fig. 2, we predict the time-integrated antineutrino energy spectrum weighted by the IBD cross section. As can be seen, the fast neutron induced fission antineutrino spectrum is a factor of about 1.2 higher in magnitude than the 14 MeV spectrum. In the right panel, we compare the spectral shapes of the fast and 14 MeV spectra. To make this comparison, we integrated over several different windows in time (indicated by color) and we then normalize each time-integrated spectrum such that its integral over energy is equal to one. The extracted normalization is then the total number of neutrinos emitted in that particular window of time. The normalized spectrum (denoted $d\tilde{N}_{\bar{\nu}}/dE_{\bar{\nu}}$) is then plotted for the fast neutron induced fissions (solid lines) and for the 14 MeV neutron induced fissions (dashed lines). We observe in this figure that the spectra are nearly identical implying that it is challenging to leverage information about the spectral shapes independently of the overall normalizations of the spectra to discriminate between the energies of the neutrons which induced the fission events. We have tabulated the extracted normalizations and present them in Table I.

An IBD detector is ultimately sensitive only to neutrinos with energies above the IBD threshold of approximately 1.8 MeV. The total number of events seen by the detector between times t_0 and t_1 is proportional to the spectrally averaged IBD cross section $\bar{\sigma}$.

$$\bar{\sigma}[t_0, t_1] = \int_{t_0}^{t_1} dt \int_{E_{\bar{\nu}}} dE_{\bar{\nu}} \frac{d^2 N_{\bar{\nu}}(t, E_{\bar{\nu}})}{dE_{\bar{\nu}} dt} \sigma_{\text{IBD}}(E_{\bar{\nu}}) \quad (1)$$

Assuming no variation in the total neutrino flux across the volume of the detector which is situated a distance R from the prompt fission event (e.g. a nuclear explosion), the total number of detected IBD events in a window of time $([t_0, t_1])$ is then

$$N_{\text{IBD}} = N_p N_f \frac{\bar{\sigma}[t_0, t_1]}{4\pi R^2} \quad (2)$$

Here, N_p is the total number of protons in the detector and N_f is the total number of fissions which happened in the pulse. Thus, $\bar{\sigma}$ is the effective cross sectional area that the IBD detector presents to the antineutrinos from the explosion. Because the antineutrino spectrum evolves in time, $\bar{\sigma}$ will also vary through time. We have tabulated it for the same windows in time as Table I and present it in Table II.

There are two opposing effects at work in the evolution of $\bar{\sigma}$. Because β -decay is a weak decay process, the beta decay of fission fragments occurs on a much slower timescale than the fission event itself and thus there are relatively few antineutrinos emitted at early times. However, the early-time antineutrinos carry a higher energy on average than those at later times. Because the IBD cross section above the reaction energy threshold is an increasing function of energy, $\bar{\sigma}$ rises to a peak value after approximately 10 seconds and then falls as both the antineutrino emission rate and average antineutrino energy fall. We have tabulated the falling average antineutrino energy in Table III for the same time windows. We have not accounted for the effect of antineutrino flavor oscillations in this analysis, as the oscillation probability depends on the distance R which we take as a free parameter in this discussion. The values presented here are therefore an upper bound on the detector response, and a more careful treatment applicable to a specific detector would need to take the disappearance of $\bar{\nu}_e$ through flavor oscillations into account by weighting the integrand of eq. 1 by the energy and distance dependent $\bar{\nu}_e$ survival probability.

In extracting the number of fissions from a neutrino measurement, we first consider the scenario in which there is no independent measurement/knowledge of the 14 MeV neutron yield, except from a simulation prediction of unknown

	0.0-0.1 s	0.1-1.0 s	1.0-10.0 s	10.0-100.0 s	100.0-1000.0 s	Total
$\bar{\sigma}$ (Fast)	0.077	0.515	1.603	1.375	0.666	4.236
$\bar{\sigma}$ (14 MeV)	0.072	0.460	1.288	0.991	0.540	3.351

TABLE II. The spectrally averaged and time integrated IBD cross section in units of 10^{-43} cm² (denoted $\bar{\sigma}$) for ²³⁹Pu. These are obtained by weighting the time-integrated spectra for the time windows as shown in figure 2 by the IBD cross section and the normalization of Table I and integrating over the energy. To calculate the experimentally measured number of IBD events, multiply $\bar{\sigma}$ by the $1/R^2$ area normalized number of fission decays, number of free H atoms, and detection efficiency. Note that $\bar{\sigma}$ already contains the IBD 1.8 MeV threshold efficiency.

	0.0-0.1 s	0.1-1.0 s	1.0-10.0 s	10.0-100.0 s	100.0-1000.0 s
$\langle E_{\bar{\nu}} \rangle$ (Fast)	2.842	2.765	2.522	2.042	1.587
$\langle E_{\bar{\nu}} \rangle$ (14 MeV)	2.871	2.773	2.495	1.988	1.581

TABLE III. Average energy of the emitted antineutrinos from fast (top row) and 14 MeV (bottom row) neutron induced fission of ²³⁹Pu across all energies in the specified time window in units of MeV.

accuracy. We also assume that the sole actinide fissioning is ²³⁹Pu. The predicted measured neutrino spectrum in Fig. 2 is the sum arising from fast and 14 MeV neutron-induced fission. Clearly any uncertainty in neutron fluxes will result in nuclear explosion yield errors when extrapolating from measured neutrino fluxes.

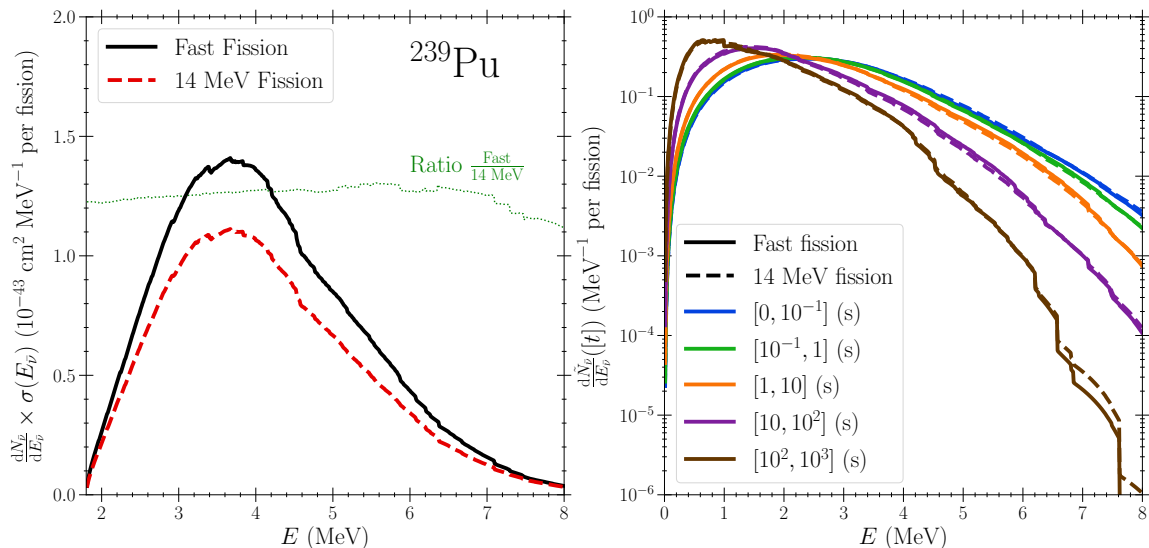


FIG. 2. (Left) The time integrated and IBD cross section weighted antineutrino spectra from neutron-induced fission of ²³⁹Pu for fast (black) and 14 MeV (red) neutrons. (Right) The antineutrino spectra for fast (solid lines) and 14 MeV (dashed lines) neutrons, integrated over five windows in time: 0-0.1 seconds (blue), 0.1-1.0 seconds (green), 1.0-10.0 seconds (orange), 10.0-100.0 seconds (purple), and 100.0-1000.0 seconds (grey). The spectra have been normalized such that the integral of the shown curve over energy is equal to 1. The extracted normalization is tabulated in table I.

2. Prompt Fission Yield Assumption

On the relatively slow timescale for neutrino emission from an nuclear explosion, the neutrinos are produced by the equivalent of a neutron pulse inducing the fission, and the shape, magnitude and timing of the spectrum is determined by the direct population and subsequent beta-decay of the fission fragments. The fission products (FP) are produced both directly in fission, with an *independent* yield (Y_i), and from the beta-decays of the more neutron rich fission products of the same mass. In order to extract the time dependent energy spectrum of antineutrinos emitted through the beta decays of the prompt FPs, we make the assumption that the FP's were populated and distributed equally to the known FP independent yields for a given fuel isotope by an approximately zero-duration event at what we

define to be $t = 0$. We then track the decays of each FP along each possible decay chain until a distribution of quasi-stable (i.e. sufficiently long lived) isotopes and isomers are populated from the initial distribution. We obtained each species' half-life ($t_{1/2}$) and decay branching ratios (b) for each decay from the RIPL-3 nuclear reaction database [17]. We determine the time-dependent yield of each species (denoted as simply $Y(Z, A, m)$) by solving a coupled, linear, initial value problem for which the instantaneous change in the time dependent yield of an isotope with atomic number Z , mass A , and isomer index m is given by

$$\frac{d}{dt}Y(Z, A, m) = -\Gamma(Z, A, m)Y(Z, A, m) + \sum_{(Z', A', m')} b(Z', A', m')\Gamma(Z', A', m')Y(Z', A', m'). \quad (3)$$

Here, $\Gamma(Z, A, m) \equiv \ln(2)/t_{1/2}$ is the decay rate of the species (Z, A, m) which has halflife $t_{1/2}$. The sum over (Z', A', m') represents the total contribution of all possible species which *decay into* the LHS species (Z, A, m) , and the factor $b(Z', A', m')$ represents the branching ratio for which the parent species undergoes the specific decay to the LHS species. The sum includes such processes as transitions between isomer states, beta decay, and beta decay with emitted neutrons.

The prompt fission assumption enters the model through the initial condition (i.e. at $t = 0$ the yields are given by the independent yields of the fissioning isotope) and the absence of a source term in eq. 3. If the fissioning material changes composition or fissioning rate on a timescale which is comparable to the typical decay rates present in eq. 3, then a source term would be included in the evolution of the yields.

The instantaneous total antineutrino energy spectrum is then the weighted sum over all of the beta decay spectra from the present decaying nuclei [18], and the weights are a product of the time dependent yield fractions determined above, the total beta decay branching ratio for the decay of each species, and each species decay rate. The total number of antineutrinos emitted ($N_{\bar{\nu}}$) per unit time is the time derivative of the energy-integrated spectrum. We plot the total number of emitted antineutrinos per second per fission in the left panel of Fig. 3. Because the decay rate is larger for higher energy antineutrinos, those emitted at earlier times have a correspondingly higher average energy, and we plot the instantaneous average antineutrino energy as the fission yield distribution evolves in the right panel of Fig. 3.

A reactor operating at steady state fissions actinide isotopes at a nearly constant rate. Once the distribution of isotopes in the reactor reaches its equilibrium state, the rate at which any individual isotope decays is equal to the rate at which it is populated both directly from fissions and from the decay of other isotopes. For unstable isotopes the value to which a yield saturates is proportional to the ratio of the steady state fissioning rate to the specie' half-life and the species *cumulative* yield. The cumulative yield is simply the sum of the independent yields of all of the isotopes in the decay chain "above" the isotope under consideration (suitably weighted by the branching ratios along the decay chain). The cumulative yields for fast and 14 MeV neutron induced fissioning of ^{239}Pu are known [19] and are utilized to model neutrino fluxes from reactors operating under equilibrium conditions [13]. Under such steady state conditions, the effective cross sections, number of neutrinos per fission, and average neutrino energy all become time independent and we provide them for ease of comparison in Tables I, II, and III. The expected number of antineutrinos from a given reactor with a known fuel composition can be calculated from the cumulative yields of the reactor fuel components and is found to be ≈ 6 for a typical Uranium power generation reactor [13]. The number of antineutrinos per fission we find for the prompt fission case is substantially lower at ≈ 2.5 (see Table I), however the spectrally weighted cross section ($\bar{\sigma}$) is of comparable magnitude: for ^{239}Pu fissioning in a reactor environment the Daya Bay Collaboration measured $\bar{\sigma} = 4.27 \pm 0.26 \times 10^{-43}$ cm² per fission [20], to be compared with Table II. In a reactor, the majority of the antineutrinos emitted are of energies below the IBD threshold and so do not produce a signal in an IBD detector resulting in an overall comparable detector response for both the reactor and nuclear explosion cases.

3. Systematic Errors in Nuclear Explosive Yield

The neutrino measurement error depends on the number of neutrino events detected (statistical), and systematic errors coming from detection threshold energy resolution and reconstruction efficiency (systematic). For statistics in the thousands of events and reasonable assumptions on systematic errors, we can expect a total error on the measured neutrino flux of about 4%, or less.

A more uncertain error comes from extrapolating the measured neutrino flux back to a test device explosive yield. A few of the assumptions were discussed above. These include errors from the prompt fission yield assumption, the detailed evolution of the neutron flux that is inducing fission, uncertainties in evaluated nuclear data and reaction libraries, and fission product database uncertainties (ENDF [17, 19]). These assumptions need to be tested and measured in a control experimental setup as described in the next section.

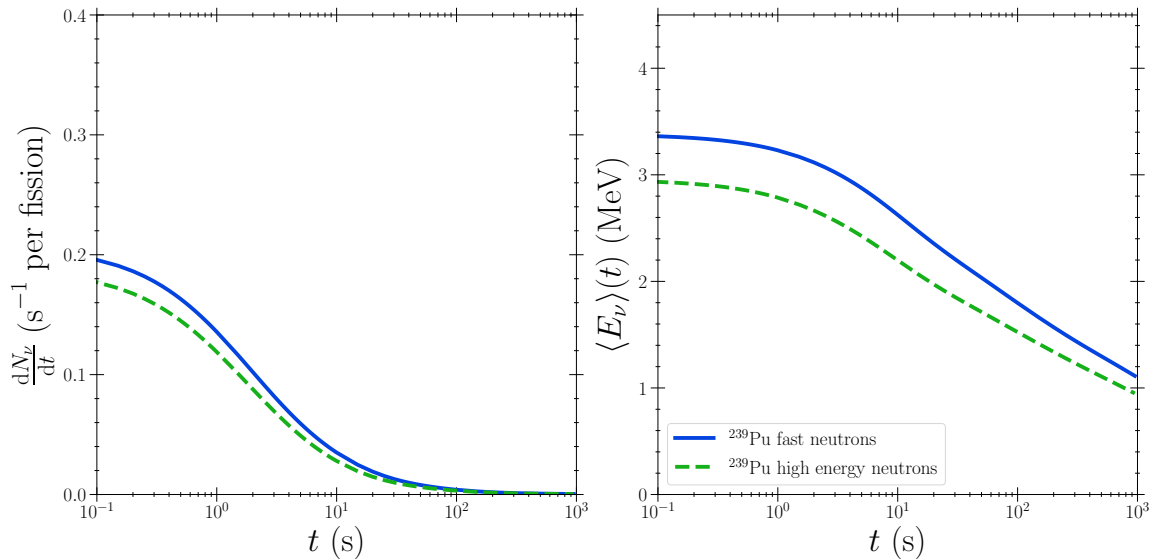


FIG. 3. The total antineutrino emission rate (left) and the instantaneous average energy (right) of neutrinos emitted by the chain of beta decays of promptly generated fission products for fast and 14 MeV induced fissions of ^{239}Pu . The legend applies to both panels.

IV. NEAR-TERM PULSED REACTOR DEMONSTRATOR EXPERIMENT

In the absence of nuclear weapons testing for the foreseeable future, many of the technical and theoretical challenges of a full nuclear test could be mitigated in the next few years with a smaller scale moderate cost demonstration detector. The plan is to deploy a 20 tons fiducial mass (25 tons total) IBD detector placed near a pulsed reactor, such as the Texas A&M TRIGA 1GW-10 millisecond pulsed facility. The short duty cycle and repeatability of pulses would provide critical real condition testing and knowledge which would be valuable for planning a possible real test shot in the future. Furthermore, the measured neutrino rate per pulse as a function of time would provide unique constraints on fission databases, equilibrium assumptions, and yield errors. Such a near-term demonstrator experiment could be funded quickly and at a reasonable cost.

Typically, a pulsed reactor can generate $\sim 10^{17}$ fissions in a single pulse, thus many pulses are needed to achieve the number of fissions required for the demonstration. By recording events triggered in a ~ 1000 seconds timing window following a reactor pulse, backgrounds can be further reduced and a decay curve of the fission products can be measurement. The close proximity of the detector and the ability offline to superimpose multiple pulses on the same pulse trigger allows an accurate simulation of the event rate pile-up in a nuclear explosion. In Section IV 1 and IV 2, we will discuss various pulsed neutron sources that we have explored and number of neutrinos that we expect to see at each facility. Section IV 3 details the technical measurements to be made and Section IV 4 will describe our preliminary detector design. The size of the detector has to allow for sufficient statistics based on the total number of fissions that we expect at each facility.

1. Pulsed Neutrino Sources

One of the pulsed reactor sources that we have identified are TRIGA reactors, which can run in steady-state and pulsed mode [21]. The TRIGA reactors can produce a brief supercritical pulse and generate a tremendous amount of neutrino flux over 10's of seconds, which is ideal for separation from the fast neutron and gamma related backgrounds and random backgrounds. The Texas A&M (TAMU) TRIGA reactor has been identified as a potential neutrino source. The 20% ^{235}U enriched reactor has a steady-state fission rate of 1-megawatt and can produce a peak power 250-megawatt pulse with a width of up to 40 ms, producing 3×10^{17} fissions per pulse [21]. The reactor also has large floor space and experimental facilities to deploy a moderate size detector as close as 4 m, including shielding, from the reactor core (see Figure 4). The pulsed reactor at Sandia National Laboratory [22] has even higher pulsed power characteristics as TAMU, greater than $\sim 1 \times 10^{18}$ fissions per pulse. We will also be investigating the logistical feasibility of mounting a neutrino detector at the Sandia pulsed reactor.

2. IBD and Background event rates at TAMU TRIGA

The expected number of fissions per pulse at the TAMU TRIGA during normal operations is 3×10^{17} fissions/pulse. Due to small neutrino rates per pulse, analysis will only take place between 0.1 and 100 seconds after a pulse to reduce steady state backgrounds (the DAQ window will still be active for at least 1000 seconds). Calculating $\bar{\sigma}$ for a prompt fissioning of ^{235}U from thermal neutrons in this time range gives $5.09 \times 10^{-43} \text{ cm}^2$. Given a detector distance of 4m (center of reactor to center of detector), and the same number of free H per detector ton from Section II, then the rate is 0.0066 neutrinos/ton/pulse (this already includes threshold efficiencies). For 2000 pulses an operation year [23], a 20-ton fiducial detector discussed below, and 80% detection efficiency (Section II), then the IBD event rate is 210 events/year. This is a small but reasonable amount of events to test the various technical challenges detecting neutrinos from a short burst. A three year run will provide a 4% statistical error on the measured pulsed power yield. Given the higher power, the event rate at Sandia could be much larger if the detector can be placed at a similar nearby distance as at TAMU, and is currently being investigated.

Shielding will be added to reduce both fast and thermal neutrons and gamma-rays from the reactor pulse. However, it is still anticipated that a significant rate will make it to the detector at such a close distance. The strategy to mitigate this prompt component is to cut out from analysis the first 100 milliseconds of data. This will result in only a 2% reduction in neutrino signal since the majority come from slower fission decays (see Table II).

Accidental backgrounds from cosmic rays (500 Hz) and PMT beta-gamma's (2 kHz) are easily rejected by veto and large charge cuts and will create an analysis dead-time of only 0.25%. Steady state background from activation and other external source of $\sim\text{MeV}$ gamma-rays is expected to be about 10 kHz (based on the 10-ton LAr CCM detector measurements at Lujan neutron source [24]). Adding appropriate shielding including borated poly (for neutron capture) and steel (for gamma absorption) should reduce this to $\sim 3.5 \text{ kHz}$, again from CCM experience. After 1.8 MeV energy threshold and fiducial cuts this can be reduced to $<100 \text{ Hz}$. Finally, accidental neutrons from cosmogenic and PMT glass sources need to be considered, but are expected to be small. At this level the accidental background rates to IBD (for a 10 micro-second neutron capture time) from external gamma-ray backgrounds is 0.1%. Using a 100 second DAQ window pulsed 2000 times is 200 events in a one year run. As this is steady state it can be measured precisely by strobe and pre-pulse data and subtracted from signal and represents a $\sim 10\%$ subtraction error on the expected signal. However, adding more shielding and improved analysis to control the rate is important to reducing the statistical error in the subtraction.

3. IBD Technical Tests Measurements at TAMU TRIGA

The primary purpose of running a IBD detector at a pulsed reactor is to test and understand the characteristics and issues related to IBD neutrino detection from a short pulsed source. In the past all IBD neutrino detector experiments have been performed at steady state reactors. The capability of these detectors have been well characterized and proven. However, a pulsed source such as an nuclear weapons test has some unique challenges. The following is a list of unique tests to be performed for a IBD detector at a pulsed reactor source,

- Most of the neutrinos arrive within 1000 seconds. The preferred run mode is an unbiased trigger (collecting all digitization data for all PMT's over the entire 1000 seconds) puts an extremely large data throughput load on the DAQ ($>1000 \text{ TBytes/pulse}$). The heavy data throughput will require new solutions such as faster readout hardware, more DAQ computers, and increased fast data storage buffer that all need to be tested and implemented. If an unbiased trigger cannot be implemented, then a event trigger based on detector activity will have to be studied and implemented. There can be a loss of physics if this is not done carefully and tested before a potential one-time shot.
- Large pile up of IBD events from a weapons test up to a 1000 second interval will present reconstruction challenges. An IBD event is identified by a prompt position then followed by a capture neutron on Gd within about 10 micro-seconds. With multiple events happening together (up to many thousands from a nuclear explosion), uniquely tagging a positron with a capture neutron becomes more difficult. At a low rate steady state reactor this is not an issue, but for an intense pulsed source it becomes critical. Any one pulse from the TRIGA reactor will have minimal overlap, but after collecting a few years worth of many pulses, these events can be overlapped to produce a data stream that mimics the intensity with a bomb. Analysis strategies can then be developed and tested before a one-time shot. A potential outcome of this study is the realization that capturing the IBD neutron with Gd will only confuse the event reconstruction and is best not added to the scintillator.

- Perform background measurements of both steady state (cosmic rays, cosmogenic neutrons, PMT U/Th activity, neutron activation, etc) and direct backgrounds from the source such as fast neutrons and gamma-rays. Develop strategies to mitigate.
- Starting with the IBD neutrino rate measurement, we will apply reactor fission codes (such as ENDF [19]) to extrapolate back to the reactor power per pulse, which is known to $\sim 1\%$ level [23]. This is important for testing the various methods and codes necessary for bomb test yield predictions using neutrino rates. From steady state reactor measurements in the past we know this error to 3-4%. The TAMU TRIGA reactor runs half the time in steady state mode which will allow a measurement of the steady state neutrino rate (this is estimated to be over 10,000 events/year, albeit with much higher background rate). Comparison of the steady state rate to pulsed mode with the same reactor and detector could yield useful information on equilibrium fission rates versus pulsed dynamics.

There is also a set of basic science measurements that can be performed parasitically to the main effort and is described in Section IV 6.

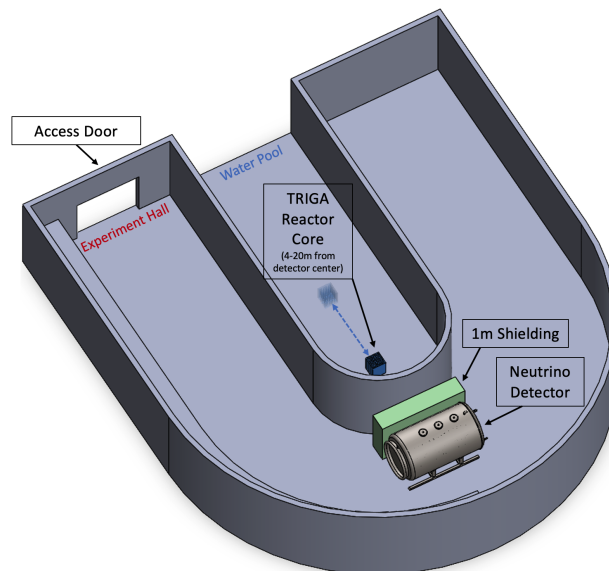


FIG. 4. The 20-ton (fiducial) mass ν FLASH detector situated at the TAMU TRIGA reactor. There is sufficient space to place the detector as close as 4 m from the movable reactor and allowing 1 m of shielding (combination of borated poly, concrete, and steel). If required, the detector can be placed further away from the reactor to allow more shielding. There is sufficient facility infrastructure (power, cooling, etc) to mount the experiment effectively.

4. IBD Test Detector Design (ν FLASH)

To achieve the estimated 630 IBD neutrino event interactions in three years of pulsed running at the TAMU TRIGA reactor requires at least 20-ton fiducial mass (see calculations above). Due to mass losses in the outer veto regions and lack of efficiency, a detector with 25-tons total mass is required. The detector is to be filled with the commercially available EJ-335 scintillator oil doped with Gd [14]. This oil has proven high scintillation light output of 9600 photons/MeV of deposited energy and a thermal neutron capture time of 5.5 microseconds for a Gd concentration of 0.5% (~ 30 microseconds for 0.1% Gd concentration). The higher the Gd concentration the shorter the capture time and better background rejection from the positron-neutron coincidence.

The detector physical design (see Figure 5) is based on the successful Coherent Captain-Mills (CCM) experiment which is performing accelerator-based sterile neutrino, dark matter, and axion searches at LANSCE Lujan center [24–26]. Even though the CCM experiment is liquid argon based, the physical structures, PMT’s, electronics, data analysis, and simulations will share many of the physics features of the ν FLASH detector. This will save an enormous amount of design time and experimental effort based on a proven sensitive detector concept. Figure 5 shows a solidworks design for the detector that is 20’ long by 8.5’ diameter (25-tons oil). The diameter is chosen to be transportable on a flat bed truck so it can be conveniently built at LANL then sent to TAMU, or elsewhere should future sources be envisioned.

We plan to use up to 500 standard 8" diameter PMT's which have 22% quantum efficiency around 400 nm to detect the scintillation and Cherenkov light produced by the neutrino final state particle interactions (position and neutron capture gamma-rays). These will be instrumented with CAEN V1730 (500 MHz 14 bit charge ADCs) which will measure the neutrino interaction light pulses to nano-second time resolution and better than 5% charge resolution.

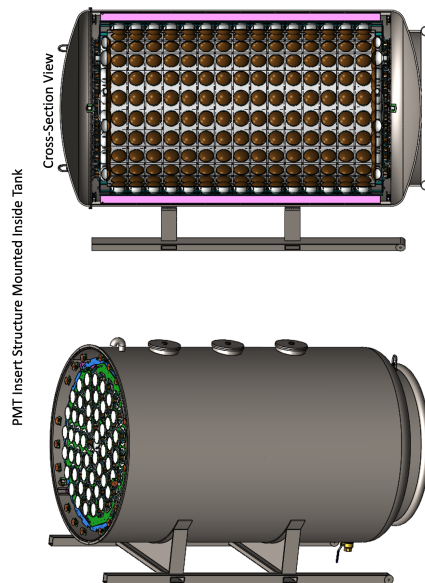


FIG. 5. The pulsed reactor ν FLASH test detector design. A total of 25-ton mass (8.5' diameter and 20' length) of gadolinium doped mineral oil (EJ-335) and instrumented with up to 500 8" PMTs. The fiducial volume for efficient neutrino detection is 20-tons. Most of the physical components have been proven with CCM and detection methods proven by other reactor neutrino experiments.

5. Detector Simulation Results

Preliminary simulations of the ν FLASH mineral oil detector have been completed to show the feasibility of this method. Initial simulations used the existing CCM geometry [26, 27] and Geant4 [28] framework to test the ability of such a detector to identify IBD coincidence between the initial positron and the successive neutron capture.

The simulation used Gd-doped EJ-335 mineral oil at various concentrations. The mineral oil filled a cylindrical detector with 200 internal PMTs facing a 7-ton fiducial volume. An incident neutrino spectrum was convoluted with the IBD capture cross section to produce an event spectrum. These events consisted of $n+e^+$ generated simultaneously with appropriate energy/momentum from a neutrino IBD event. Both initial particles were then allowed to propagate using the FTFP_BERT_HP physics list and Geant4 optical physics built from the properties of EJ-335 mineral oil scintillator [14]. Detection occurred through optical photon interaction with models of the current CCM PMTs built from LED-based single photo-electron (SPE) and radioactive source-based efficiency calibrations [26, 27].

The simulation produced expected results - see Figure 6. 100% of initial positrons were detected to some level, although not all were fully captured within the fiducial volume. The positron spectrum peaked at ~ 3000 PEs (photo-electrons, a measure of reconstructed energy), indicating a true/reco energy ratio of 1 MeV to 1250 PEs. This gives the simulated detector sensitivity to energies between 0.01 and 30 MeV before PMT pileup becomes an issue. Approximately 80% of neutrons captured within a 10 μ s window at 1% Gd doping, while another simulation using 0.5% doping only captured $\sim 35\%$ within the same 10 μ s window. A ~ 5 μ s thermalization time preceded the expected thermal neutron capture time of 5.5 μ s. The majority of these captures were on Gd-155 or Gd-157 in both cases, producing a cascade of gamma-rays totalling approximately ~ 8 MeV. This was reconstructed in the expected energy region similar to the positron spectrum, between 8 and 10,000 PEs. The positron's reconstructed time is taken as the neutrino arrival time since the positron is produced immediately after interaction. The neutrino energy is taken as the reconstructed positron energy plus 1.8 MeV due to interaction threshold. The energy resolution on the reconstructed

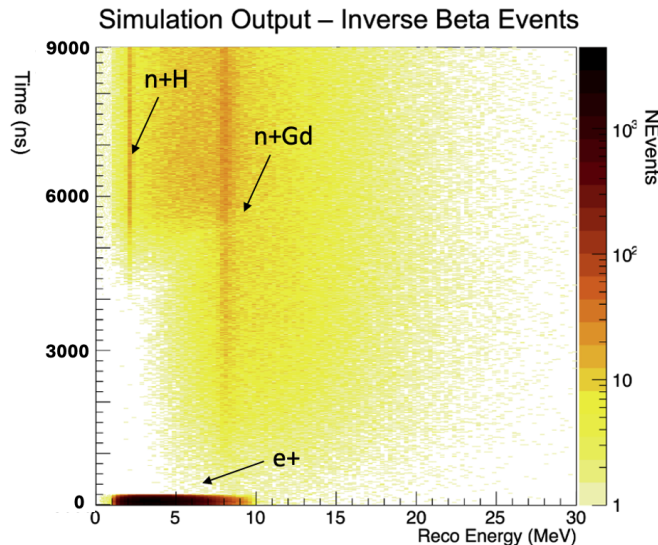


FIG. 6. The reconstructed time and energy output of the IBD simulation in the ν FLASH detector. At the bottom left, in dark red, is the fast positron scintillation peaking at ~ 2.4 MeV. The large cloud that dominates the figure is the delayed neutron captures out to 9 μ s after the positron. The majority of such captures are Gd-captures producing 8 MeV of gammas. A minority are hydrogen captures producing 2.2 MeV, producing a line above the positron cluster.

positron is about 5% within the fiducial volume. This can be further reduced with advanced reconstruction techniques such as charge-time log-likelihood reconstruction analysis.

6. Additional Fundamental Science Drivers

Parasitic to testing technical capabilities of an IBD detector at the TAMU TRIGA pulsed source for weapons physics, there are a number of basic science measurements that can be pursued in parallel. This has the added benefit of attracting university collaborators and students to participated in the open science and help make the overall project a success. The not complete list of science measurements are,

- Investigate the source of the ~ 5 MeV bump in the reactor neutrino spectrum observed at steady state reactor experiments [29]. Measuring the time profile might yield information on the fission source responsible for the bump, though statistics in the region of interest will be a challenge.
- The energy and baseline of the ν FLASH experiment is ideal to test for sterile neutrino oscillations at $L/E \sim 1$ region [30]. This could provide a direct measurement of neutrino oscillations consistent with Neutrino-4 and BEST results [31, 32] that have found significant evidence for $\bar{\nu}_e$ or ν_e disappearance. With a planned three year run, Figure 7 shows the anticipated reach of ν FLASH to search for large Δm_{14}^2 $\bar{\nu}_e$ disappearance oscillations consistent with the Neutrino-4 and BEST signals. With 2000 pulses per year, we anticipate 210 unoscillated IBD neutrinos/year after efficiency as discussed previously in Section IV 2. Due to the compact and movable reactor core, ν FLASH can perform a sensitive L/E shape analysis where many of the large systematic errors from neutrino flux and cross section only affect normalization, not shape, to first order. Also, due to the short source pulsing and IBD signal coincidence, backgrounds will be mitigated significantly and are assumed to be small - the sensitivity plot in Fig 7 includes 10% background subtraction error (see subsection IV 2 for details). Further details of the experiment and sensitivities will be presented in a future physics paper. The irony here is if sterile neutrinos at the $\Delta m_{14}^2 \sim 1eV^2$ do exist, they would become the largest systematic error in nuclear weapons yield extrapolation from neutrino rate measurements.
- A pulsed reactor produces a large number of gamma-rays and electrons that can couple to axions. Recent models have demonstrated the ~ 1 MeV region as a motivated place to search [33]. The prompt time production of axions in the reactor core will help separate it from the IBD neutrinos coming from the slower fission decays, but will still have to contend with large prompt backgrounds from the beam neutrons and gamma-rays. The limited pulsing of the reactor will reduce signal rate, but the significant random background rejection due to

the pulse timing will improve overall sensitivity. Sensitivity calculations are on-going and will be reported in a future paper.

- Electromagnetic and gravitational waves currently underpin the multi-messenger era in astrophysics. These signals can disentangle the masses of stars associated with compact object collisions [34], provide insight into the nuclear equation of state [35], and indicate the production of heavy elements in explosive events [36, 37]. Neutrinos offer a third, complementary perspective on astrophysical events, giving insight into numerous processes. Because neutrinos can escape the interiors of astrophysical environments, they allow observation of internal mechanisms and conditions [38]. Precision energy- and time-resolved measurements of pulsed neutrinos in terrestrial environments, as suggested in this paper, will help to refine the prediction of neutrino signals for astrophysics. A well characterized neutrino signal can enhance understanding of astrophysical nuclear processes. Neutrino measurements can provide constraints on standard model physics and extensions thereto, which directly affect the evolution of extreme astrophysical environments.

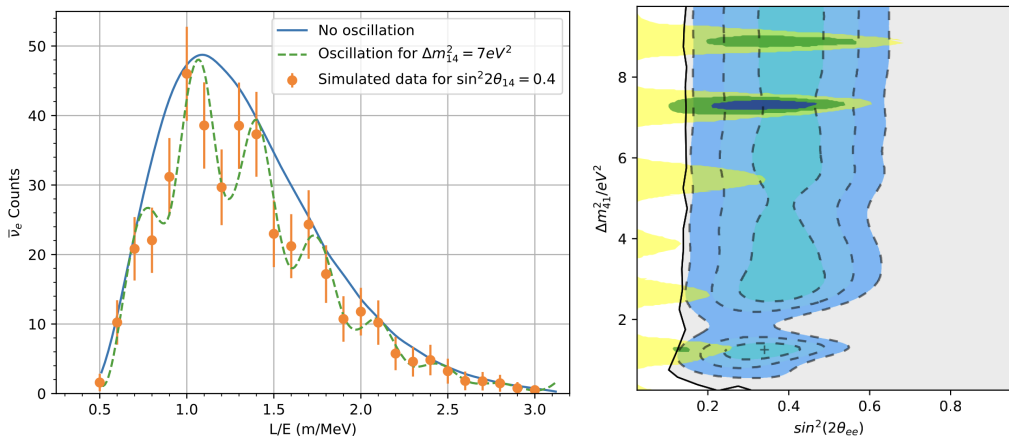


FIG. 7. Left: Simulated ν FLASH 20-ton IDB detector neutrino L/E distribution after three years of running at the TAMU pulsed reactor at a distance of 4 m from the source. Error bars are statistical only, no backgrounds, and assumes $\Delta m_{14}^2 = 7eV^2$ and $\sin^2 2\theta_{14} = 0.4$ (near Neutrino-4 best fit). Smearing effects include source size, IDB energy spectrum, 5% energy and 10 cm position resolution. Right: Three year 90% confidence limits sensitivity for ν FLASH (solid line and grey region) covering the signal regions from Neutrino-4 (Yellow) and BEST (Blue).

V. CONCLUSIONS

Due to neutrinos prolific production in fission reactions during a nuclear weapons test, they can be used as a novel and complementary tool for diagnostics. With large fiducial mass and prolific scintillation light detection, the modern neutrino detector using the IBD reaction can easily detect thousands of neutrinos from a stand off distance of 500 meters. Should the U.S. ever go back to nuclear weapons testing, the use of neutrinos would provide a new tool to better understand and diagnose the performance of a weapon. In the mean time, the technology and methods used can be tested at a pulsed reactor such as the TAMU TRIGA reactor, which is a good surrogate for a nuclear weapons test. This enables studying yield extraction, non-equilibrium fission rates, and systematic errors. As well, tests can be performed of the neutrino detector technology in a pulsed environment, such as neutrino pileup, readout rates, triggering, etc. Finally, with a modest sized 20-ton fiducial mass scintillation detector (ν FLASH) deployed at a pulsed reactor, tests of the Neutrino-4 and BEST disappearance signal can be performed, which could be indication of sterile neutrino oscillations at the $\sim 1eV^2$ scale. Using a reactor in pulsed mode for neutrino physics is novel and would yield significant background reduction and enable the study of the time evolution of fission neutrinos. Such a rich program is of modest cost and could be deployed in a few years.

VI. ACKNOWLEDGEMENTS

We thank Prof. B. Dutta (TAMU) and I. Bisset (TAMU) for physics discussions and generating the sterile neutrino sensitivity plots in Figure 7. This document has been reviewed and has LANL library reference number LA-UR-24-29431.

-
- [1] F. Reines and C. L. Cowan. A proposed experiment to detect the free neutrino. *Physical Review*, 90:492, 5 1953.
- [2] Los Alamos. The reines-cowan experiments: Detecting the poltergeist. *Los Alamos Science*, 25:3, 1997.
- [3] C. L. Cowan, F. Reines, F. B. Harrison, H. W. Kruse, and A. D. McGuire. Detection of the free neutrino: a confirmation. *Science*, 124:103–4, 7 1956.
- [4] P. A. Zyla et al. Review of Particle Physics. *PTEP*, 2020(8):083C01, 2020.
- [5] Alison Abbott. The singing neutrino nobel laureate who nearly bombed nevada. *Nature*, 593:334–335, 5 2021.
- [6] Xin Qian and Jen-Chieh Peng. Physics with Reactor Neutrinos. *Rept. Prog. Phys.*, 82(3):036201, 2019.
- [7] Y Kim. Detection of Antineutrinos for Reactor Monitoring, Nuclear Engineering and Technology, 48, Issue 2, pg 285-292, 2016.
- [8] Patrick Huber. On the determination of anti-neutrino spectra from nuclear reactors. *Phys. Rev. C*, 84:024617, 2011. [Erratum: *Phys.Rev.C* 85, 029901 (2012)].
- [9] Ll. Marti et al. Evaluation of gadolinium’s action on water Cherenkov detector systems with EGADS. *Nucl. Instrum. Meth. A*, 959:163549, 2020.
- [10] F. P. An et al. The Detector System of The Daya Bay Reactor Neutrino Experiment. *Nucl. Instrum. Meth. A*, 811:133–161, 2016.
- [11] H. de Kerret et al. The Double Chooz antineutrino detectors. *Eur. Phys. J. C*, 82(9):804, 2022.
- [12] Anna Hayes and Josh Martin (LANL T-2). *Simulation estimate*.
- [13] Anna C. Hayes and Petr Vogel. Reactor neutrino spectra. *Annual Review of Nuclear and Particle Science*, 66(1):219–244, 2016.
- [14] Eljen Technology (EJ-335), <https://eljentechnology.com/products/liquid-scintillators/ej-331-ej-335>.
- [15] Feng Peng An, Akif Baha Balantekin, Henry Reyer Band, M Bishai, Simon Blyth, D Cao, Guo Fu Cao, Jun Cao, WR Cen, Yat Long Chan, et al. Improved measurement of the reactor antineutrino flux and spectrum at daya bay. *Chinese Physics C*, 41(1):013002, 2017.
- [16] Shin Okumura, Toshihiko Kawano, Amy Elizabeth Lovell, and Tadashi Yoshida. Energy dependent calculations of fission product, prompt, and delayed neutron yields for neutron induced fission on 235u, 238u, and 239pu. *Journal of Nuclear Science and Technology*, 59(1):96–109, 2022.
- [17] Roberto Capote, Michel Herman, P Obložinský, PG Young, Stéphane Goriely, T Belgya, AV Ignatyuk, Arjan J Koning, Stéphane Hilaire, Vladimir A Plujko, et al. Rip1–reference input parameter library for calculation of nuclear reactions and nuclear data evaluations. *Nuclear Data Sheets*, 110(12):3107–3214, 2009.
- [18] We have further assumed that all considered beta decays are allowed. A more detailed analysis including shape factor corrections to forbidden decays will be presented in a future work.
- [19] M.B. Chadwick, M. Herman, P. Obložinský, et al. ENDF/B-VII.1 nuclear data for science and technology: Cross sections, covariances, fission product yields and decay data. *Nuclear Data Sheets*, 112(12):2887 – 2996, 2011. Special Issue on ENDF/B-VII.1 Library.
- [20] F. P. An et al. Evolution of the Reactor Antineutrino Flux and Spectrum at Daya Bay. *Phys. Rev. Lett.*, 118(25):251801, 2017.
- [21] TRIGA Reactor Characteristics, <https://ans.iaea.org/Common/documents/Training/TRIGA>
- [22] Edward J. Parma Jr. and Michael Warren Gregson. The Annular Core Research Reactor (ACRR) Description and Capabilities. <https://www.osti.gov/servlets/purl/1761930> (2019).
- [23] TAMU TRIGA Management. *Communicated estimate*.
- [24] A. A. Aguilar-Arevalo et al. First dark matter search results from Coherent CAPTAIN-Mills. *Phys. Rev. D*, 106(1):012001, 2022.
- [25] A. A. Aguilar-Arevalo et al. First Leptophobic Dark Matter Search from the Coherent–CAPTAIN-Mills Liquid Argon Detector. *Phys. Rev. Lett.*, 129(2):021801, 2022.
- [26] A. A. Aguilar-Arevalo et al. Prospects for detecting axionlike particles at the Coherent CAPTAIN-Mills experiment. *Phys. Rev. D*, 107(9):095036, 2023.
- [27] Dunton, Edward C. A search for axion-like particles at the coherent captain mills experiment (<https://doi.org/10.7916/x9x1-ka48>). 2022.
- [28] Geant4 Physics Simulation Code. *NIM A 506 (2003)*, pg 250.
- [29] Patrick Huber. NEOS Data and the Origin of the 5 MeV Bump in the Reactor Antineutrino Spectrum. *Phys. Rev. Lett.*, 118(4):042502, 2017.
- [30] Petr Vogel, Liangjian Wen, and Chao Zhang. Neutrino Oscillation Studies with Reactors. *Nature Commun.*, 6:6935, 2015.
- [31] A. P. Serebrov et al. Search for sterile neutrinos with the Neutrino-4 experiment and measurement results. *Phys. Rev. D*, 104(3):032003, 2021.
- [32] V. V. Barinov et al. Search for electron-neutrino transitions to sterile states in the BEST experiment. *Phys. Rev. C*, 105(6):065502, 2022.
- [33] James B. Dent, Bhaskar Dutta, Doojin Kim, Shu Liao, Rupak Mahapatra, Kuver Sinha, and Adrian Thompson. New Directions for Axion Searches via Scattering at Reactor Neutrino Experiments. *Phys. Rev. Lett.*, 124(21):211804, 2020.
- [34] B. P. Abbott et al. Gravitational waves and gamma-rays from a binary neutron star merger: Gw170817 and grb 170817a. *The Astrophysical Journal Letters*, 848(2):L13, oct 2017.

- [35] Francisco Hernandez Vivanco, Rory Smith, Eric Thrane, Paul D. Lasky, Colm Talbot, and Vivien Raymond. Measuring the neutron star equation of state with gravitational waves: The first forty binary neutron star merger observations. *Physical Review D*, 100(10), nov 2019.
- [36] Brian D. Metzger. Kilonovae. *Living Reviews in Relativity*, 23(1), dec 2019.
- [37] Oleg Korobkin, Aimee M. Hungerford, Christopher L. Fryer, Matthew R. Mumpower, G. Wendell Misch, Trevor M. Sprouse, Jonas Lippuner, Rebecca Surman, Aaron J. Couture, Peter F. Bloser, Farzane Shirazi, Wesley P. Even, W. Thomas Vestrand, and Richard S. Miller. Gamma rays from kilonova: A potential probe of r-process nucleosynthesis. *The Astrophysical Journal*, 889(2):168, feb 2020.
- [38] G Wendell Misch, Yang Sun, and George M Fuller. Neutrino spectra from nuclear weak interactions in sd-shell nuclei under astrophysical conditions. *The Astrophysical Journal*, 852(1):43, 2018.